Strongly Coupled Nickel-Cobalt Nitrides/Carbon Hybrid Nanocages with Pt-like Activity for Hydrogen Evolution Catalysis

*Jianping Lai[#], Bolong Huang[#], Yuguang Chao[#], Xu Chen and Shaojun Guo**

Dr. J. Lai, Prof. S. Guo
BIC-ESAT, College of Engineering, Peking University, Beijing 100871, China.
E-mail: guosj@pku.edu.cn

Dr. J. Lai, Y. Chao, Prof. S. Guo
Department of Materials Science and Engineering, College of Engineering, Peking University, Beijing 100871, China.

Y. Chao
State Key Laboratory of Coal Conversion, Institute of Coal Chemistry, Chinese Academy of Sciences, Taiyuan, 030001, China.

Prof. B. Huang
Department of Applied Biology and Chemical Technology, The Hong Kong Polytechnic University, Hung Hom, Kowloon, Hong Kong SAR.

Prof. X. Chen
State Key Laboratory of Chemical Resource Engineering, Beijing University of Chemical Technology, Beijing 100029, China.

[#]Equal Contribution

Keywords: metal nitride; nanocages; carbon; MOFs; electrocatalysis

Abstract: Designing nonprecious catalysts with comparable mass activity to state-of-art noble catalysts for the hydrogen evolution reaction (HER) in alkaline solution still remains a significant challenge. Herein we rationally design a new strongly coupled nickel–cobalt nitrides/carbon complex nanocage (NiCoN/C nanocage) *via* chemical etching of ZIF-67 nanocubes with $Ni(NO_3)_2$ under sonication at room temperature, following by nitridation. The as-prepared strongly coupled NiCoN/C nanocages exhibit a mass activity of 0.204 mA/μg at an overpotential of 200 mV for HER in alkaline solution, which is comparable to that of the commercial Pt/C (0.451 mA/μg). The strongly coupled NiCoN/C nanocages also possess superior stability for HER with negligible current loss under the overpotentials of 200 mV for 10 h. DFT calculations reveal that the excellent HER performance under alkaline condition arises from the robust $Co^{2+} \rightarrow Co^0$ transformation achieved by strong (Ni, Co)-N bonding induced efficient *d-p-d* coupled electron transfer, which is a key for optimal initial

water adsorption and splitting. High degree of amorphization urges the C-sites to be an electron-pushing bath to promote the inter-layer/sites electron-transfer with loss of orbital-selection-forbidden-rule, which uniformly boosts the surface catalytic activities up to a high level independent to the individual surface active sites.

Increasing concerns about serious energy and environmental problems urge the researcher to seek for renewable energy sources as substitutes to traditional fossil fuels.[1-4] Hydrogen that is a green energy carrier with high energy density is a hopeful substitute to fossil fuels.[5-12] Among diverse routes to hydrogen production, electrochemical water splitting has appeared as a promising route due to its simplicity, low cost, zero greenhouse gas emission and high energy conversion efficiency.[13-19] Therein, the basic hydrogen evolution reaction (HER) is deemed to be more valuable process than acidic oxygen evolution reaction due to the lack of electrocatalysts for the acidic oxygen evolution reaction. Therefore, developing HER electrocatalysts with high activity and superior stability in alkaline media is highly desirable for electrochemical water splitting because the basic HER rate is 2–3 orders of magnitude lower than that in acidic solutions.[20-30]

Currently, state-of-the-art HER electrocatalysts in alkaline solutions are precious Pt-based materials, which extremely limit their widespread commercialization. Recently, great efforts have been devoted to enhancing the performance of inexpensive electrocatalysts to replace the precious Pt-based catalysts. Among the potential catalysts, transition metal nitrides, especially nickel-based mixed metal compounds, have been widely demonstrated as highly active HER catalysts in alkaline solution owing to their special properties such as low electrical resistance, superior water dissociation kinetics and good corrosion resistance.[31-34] However, it is still a great challenge to design strongly coupled transition metal nitrides/C hybrid nanocage (NiCoN/C nanocage) structures with outstanding performance for basic HER.

In this contribution, we report a new class of strongly coupled NiCoN/C hybrid nanocages *via* reacting Co-based zeolitic imidazolate framework (ZIF-67) nanocubes with $Ni(NO_3)_2$ under sonication to create NiCo layered double hydroxide (NiCo LDH) nanoboxes, followed by low-temperature thermal ammonolysis treatment (see the Supporting Information for details). As a consequence, the strongly coupled NiCoN/C nanocages with structural and compositional benefits can show Pt-like mass activity for HER electrocatalysis in alkaline solutions. The strongly coupled NiCoN/C nanocages exhibit a mass activity of 0.204 mA/μg at an overpotential of 200 mV in 1.0 M KOH, in contrast to that of the commercial Pt/C (0.451 mA/μg). Moreover, the durability of strongly coupled NiCoN/C nanocages was also excellent under the overpotential of 200 mV for 10 h. DFT calculations reveal that the surface catalytic activities have been uniformly boosted-up to a high level independent to the individual surface active sites. Highly efficient electron-transfer *via d-p-d* coupling effect can be achievable to transform Co^{2+} to Co^0, which is a key for optimal initial water adsorption and splitting.

The schematic of the synthesis of strongly coupled NiCoN/C hybrid nanocages was depicted in **Figure 1a**. The NiCo LDH nanoboxes were first prepared by reacting ZIF-67 nanocubes with $Ni(NO_3)_2$ under sonication.[35] During the process, the protons generated from the hydrolysis of Ni^{2+} ions would chemically etch the ZIF-67 nanocubes. The Co^{2+} ions released from ZIF-67 were partially oxidized by O_2 and NO_3^- ions. Meanwhile, the amount of hydroxyl ions increased with the consumption of protons. Then the Co^{2+}/Co^{3+} ions co-precipitated with Ni^{2+} ions to form a layer of LDH around the ZIF-67 nanocubes. As the reaction progressed, the inner ZIF-67 became vulnerable, eventually leading to the formation of NiCo LDH nanoboxes. Then, the nanoboxes were chemically converted into strongly coupled NiCoN/C hybrid nanocages under a flowing NH_3 atmosphere at 350 °C for 2 h. Field-emission scanning electron microscopy (FESEM) and transmission electron microscopy (TEM) were used to characterize the morphology of the prepared ZIF-67 nanocubes. **Figure S1** shows the FESEM and TEM images of the ZIF-67 nanocubes with ca. 350 nm size. The

X-ray diffraction (XRD) analyses further reveal that the as-prepared products exclusively consist of ZIF-67 (**Figure S2**). Their further reacting with excess $Ni(NO_3)_2$ under sonication for 1 h, leads to formation of hollow LDH nanoboxes. **Figure 1b&c** show the FESEM images of the LDH nanoboxes. They still maintain the cubic shape and size. But the surfaces of products become rough. TEM images of **Figure 1d&e** further reveal that the nanoboxes are composed of nanosheets. And the thickness of the nanosheets is around 2~3 nm (**Figure 1e**). We can observe that a single LDH nanobox exhibits a dark cross contrast in the shell section compared to the regions over the inner section. This indicates that the products have hollow features. Energy dispersive X-ray (EDX) spectrum (**Figure S3**) suggests the composition of Ni and Co in LDH nanoboxes is 64/36, being in accordance with the result of ICP. The NiCoN content in strongly coupled NiCoN/C nanocages is about 76.9 wt % based on the ICP analysis. The XRD spectrum (**Figure S4**) displays the emergence of LDH phase and the vanishing of ZIF-67 phase. After the nitridation of LDH nanoboxes, porous structure on the surface of nanoboxes emerges (**Figure 2a**). TEM image (**Figure 2b**) of nanocages further manifests their porous feature on the surface of nanocages. EDX mapping images of strongly coupled NiCoN/C nanocages reveal that Ni, Co, N and C are uniformly distributed within the nanostructures (**Figure 2c**). The XRD spectrum (**Figure S5**) displays that the peaks of product are in accordance with that of Ni_3N (JCPDS no. 10-0280) or $Ni_{3-x}Co_xN$. High-resolution TEM (HRTEM) image in **Figure S6** exhibits lattice fringe spacings of 2.16 Å and amorphous region, corresponding to (002) plane of NiCoN and carbon, respectively. These results further demonstrate the successful preparation of strongly coupled hybrid nanocages.

In addition, X-ray photoelectron spectroscopy (XPS) was utilized to examine the surface state of sample. In the Co 2p XPS spectrum (**Figure S7a**), the two peaks at 778.1 eV and 794.3 eV are accordingly assigned to Co^0.[36] The peak at 779.8 eV and 795.2 eV are ascribed to the Co-N bonds in Co_3N based on literature reported data.[37] The other two peaks (781.1 and 797.3 eV) are also assigned to CoO, which arises from the surface oxidization of the sample *via* attaching intermediate

hydroxyl group or physically adsorbed water molecule when exposed to air before measurement. Meanwhile, two sharp peaks at around 853.1 and 871.0 eV (**Figure S7b**) belong to Ni 2p in Ni_3N.[34] The other two peaks at 855.0 and 872.9 eV originate from NiO by partial oxidization, which is consistent with literatures **[(1) J. Am. Chem. Soc., 2015, 137, 4119–4125; (2) Chem. Mater. 2004, 16, 4216-4225; (3) Chem. Mater. 2008, 20, 3360–3367; (4) Adv. Mater., 2018, 30, 1803367**]. The binding energy of N 1s in metal-N is 397.9 eV.[37] The higher binding energy (~0.4 eV) of N 1s in our catalysts (**Figure S7c**) is related to the electron-deficient characters in metal-N, indicating an evident electron transfer in (Ni, Co)-N bonds.

We further evaluated the catalytic properties of different catalysts towards HER in 1.0 M KOH. **Figure 3a** shows the polarization curves of Pt/C, NiCo LDH nanoboxes and strongly coupled NiCoN/C nanocages with IR compensation. The overpotential of strongly coupled NiCoN/C nanocages at 10 mA cm^{-2} is 103 mV, higher than that of the Pt/C (91 mV). However, with increasing the current density, the results show that the strongly coupled NiCoN/C nanocages only need an overpotential of 142 mV *versus* reversible hydrogen electrode (RHE) to gain a current density of 20 mA cm^{-2}, much lower than that of LDH nanoboxes and 34 mV lower than that of Pt/C (**Figure 3b)**. At the overpotential of 200 mV, the TOF of the strongly coupled NiCoN/C nanocages and Pt/C reaches 0.093 s^{-1} and 2.28 s^{-1}, respectively (**Figure S8**). Especially, the strongly coupled NiCoN/C nanocages possess a mass activity of 0.204 mA/$\mu g_{cat.}$ at an overpotential of 200 mV, comparable to that of the commercial Pt/C (0.451 mA/$\mu g_{cat.}$) (**Figure 3c)**. The H_2 production was further analyzed by gas chromatography, which shows that the detected amount H_2 gas is consistent with the theoretical value, corresponding to a Faradaic efficiency of ~100% (**Figure S9**).

We further evaluated the stability of the strongly coupled NiCoN/C nanocages and Pt/C at overpotential of 200 mV (**Figure 3d**). After 10 h test, 98.1% of the current was maintained for the strongly coupled NiCoN/C nanocages, whereas only 87% of the current was kept for Pt/C. The strongly coupled NiCoN/C nanocages also showed excellent stability during the long-time HER

measurement at the current density of 20 mA cm^{-2} with only a slight deactivation during the complete 60 h operation (**Figure S10**). The electrochemical aging test was conducted with 1000 cyclic voltammetry (CV) cycles to further check the stability of strongly coupled NiCoN/C nanocages (**Figure 3e**). There is almost no HER polarization curve shift for strongly coupled NiCoN/C nanocages after 1000 cycles, demonstrating their superior stability. In addition, there are almost no composition changes (**Figure S11a**) and reasonably retain the overall structure (**Figure 3f & S11b**) after stability test, further suggesting the excellent stability of strongly coupled NiCoN/C nanocages. Further analysis of XPS spectrum after stability test for Co and Ni 2p signal indicates that Co still maintains at zero valence state while CoN (**Figure S12a**) and the surface Ni-oxidation continues (**Figure S12b**) during the HER process. This contrasting variation arises because the dominant C parts protect the partial Co surface from direct interactions with exposed to the alkaline electrolyte, and also maintain a high current density. Thus the Co has been prevented form complete oxidations by such sacrificial agent. The competing trend of desorption of hydroxyl group favors on the Co, owing to a lower binding energies and band centers. This has been also reflected by our XPS spectra (**Figure S7** and **Figure S12**). Consistent with Xie et al [**J. Am. Chem. Soc., 2015, 137, 4119–4125**], local NiO or other hydrated nickel oxides motifs have been rarely detected, giving solid evidence that the major targeting phase still remains as NiCoN (**Figure S12c**).

We further investigate the origin of high performance HER catalysis of NiCoN/C nanocages in alkaline solution. We found that relative to LDH nanoboxes (1.09 mF cm^{-2}), the strongly coupled NiCoN/C nanocages have much higher electrochemical double-layer capacitance (EdlC) (5.1 mF cm^{-2}) (**Figure S13**), revealing the higher electrochemical active surface area (ECSA) of the strongly coupled NiCoN/C nanocages. In addition, electrochemical impedance spectra (EIS) were used to investigate the interfacial properties of catalysts (**Figure S14**). The impedance of strongly coupled NiCoN/C nanocages is much lower than that of LDH nanoboxes. Both of them can contribute to the enhanced HER electrocatalytic activity of NiCoN/C nanocages.

DFT calculations were further used to reveal the exact reason why NiCoN/C nanocages show very high HER catalysis in alkaline solution. The surface of the NiCoN-C model clearly exhibits the absence of long-range order with slightly stressed originated by the lattice distortions deviated from their crystal structure. In the NiCoN part, the Ni and Co sites evenly distributed throughout the lattice mixed with metallic bonds and nitride-bonds. This has been overall stably interfaced with amorphous C-layer for NiCoN-C system (**Figure 4a**). The electronic bonding and anti-bonding orbitals near the Fermi level (E_F) have shown a uniformly distributed valence charges from active orbitals. This indicates a homogeneously unified surface active area responsible for rich charge-transfer ability without site-to-site steric barriers. The surface catalytic activities have been uniformly boosted-up to a high level and independent to the individual surface active sites (**Figure 4b**).

Detailed projected partial density of states (PDOSs) for the Ni and Co sites are all illustrated regarding different depths or regions. We find their overall electronic activities are varied in a complementary way (**Figure 4c & 4d**). From deep-in-depth to surface, the Ni-3d band centers have been monotonically modified from the deeply localized position (E_V-2.1 eV) to the high-lying level (E_V-0.9 eV) close to the E_F, where the E_V=0 for E_F (**Figure 4c**). The Co-3d band centers are varied from electron-deficient to the electron-rich characters, denoting an electronic modulation from Co^{2+} to Co^0 states from deep bulk region to the surface top layer, respectively. From this transition, the Co-3d bands centers are modulated from E_V-0.7 eV to E_V-1.9 eV. This tendency implies that, with a strong (Ni, Co)-N bonding, highly efficient electron-transfer *via* d-p-d orbital coupling effect can be achievable. Meanwhile, mutual interactions from Ni-N and Ni-Co suppress both (Ni, Co)-3d-band activities and preserve the electron-rich character in deeper range (**Figure 4d**).

To illustrate the contribution of C-2p band, we find the C-layer does not lower the electronic activities of NiCoN layer. The overall (Ni, Co) d-band centers are almost unchanged with and without the C-layer. In addition, the gap between p- and d- band edge has been narrowed from 3.44 eV to 2.33 eV, indicating C-layer as an electron-pushing bath. Meanwhile, owing to high degree of

amorphization, local disordered lattice urges the C-2p band to present an extra widened character which promotes the inter-sites electron transfer with loss of orbital-selection-forbidden-rule. From the stably combined amorphous C-layer interface, some mutual layer diffusions have been evidently observed between (Ni, Co) ions and C sites, denoting the strong binding between NiCoN and C systems (**Figure 4e**).

We further analyze different p-band interplays from N, C, and O. The N-2p band from the surface mainly covers from Ev-3.8 eV to Ev-6.5 eV below both Ni- and Co- 3d bands, while the p-band center from the bulk is at the level of Ev-7.0 eV. It possesses strong p-d couplings to efficiently transfer the electrons from the deep bulk layer onto the surface, and well separates mutual influence between OH^- and H_2O. The contrast of N-2p bands between bulk and surface region clearly demonstrates that the N-sites not only stabilizes the surface Ni and Co sites, but also efficiently transfers the electrons from deep layer onto the surface active region (**Figure 4f**). Further on the O-related species, we find that the O-2p orbital from H_2O molecule presents the most overlapping with the Co-3d band on the surface top layer. This arises because the first dominant peak of 2p band (*i.e.*, from Ev-2 eV to Ev-4 eV) of H_2O substantially overlaps with surface Co-3d band. Accordingly, the surface Co-sites may perform the best initial water adsorption and splitting steps. The OH^- species may be very easily desorbed from the surface and will not terminate the surface active regions by over-binding effect, since the O-2p from $*OH^-$ does not perform any overlapping with Ni- and Co-3d bands, Thus, the final products exhibit an efficient desorption without encountering any over-binding with either Ni or Co sites.

We move onto the HER pathway under alkaline condition and adsorption performance, which involves the lined-up chemical reaction heat based pathways, as well as H-formation and chemisorption energies (**Figure 5a-c**). Overall, the NiCoN-C nanocage system will perform a rather energetically favorable pathway for HER (-0.40 eV), which is nearly twice lower than the performance by NiCoN (-0.21 eV) without contribution of amorphous C-layer (**Figure 5a**). At the

initial adsorption, the system of NiCoN shows the H_2O and H adsorption to be more favorable (-0.14 eV) than the case of NiCoN-C system (-0.06 eV). However, such adsorption level nearly approaching the thermoneutral line denotes the HER reaction can be initiated at nearly the neutral water reference level. This arises because the cost for stabilizing the adsorbed H_2O has already been compensated by the H-adsorption on the (Ni, Co) sites according to our calculation. This compensation further generates even more evident energetic contrast for the fixation of the H_2O before the water splitting, which are -0.18 eV and 0.13 eV for NiCoN-C and NiCoN respectively. They also lead to an energetic gain and a barrier of 0.27 eV respectively. Without amorphous C-layer as electron-rich supporting layer, the exposed Ni and Co sites from NiCoN system potentially induce the over-binding effects, especially to the H-adsorption. Although the water splitting process favors the NiCoN surface system, it still faces the barrier of 0.45 eV for generation process of $2*H \rightarrow 2H \rightarrow H_2$. Related formation energy calculation illustrates the adsorption of H and reaction towards H_2 *via* migrating and gathering 2*H is rather energetically favorable in downhill trend (**Figure 5b**). Further chemisorption energy calculation confirms the NiCoN-C system alleviates the over-binding effect with weakened chemisorption energy compared to the NiCoN system (**Figure 5c**).

From the local structural evolution (**Figure 5d**), the stable adsorbed H is locating at either Ni or Co sites among different steps, indicating a weakened binding without energetic preference. The H_2O location is found to be staying at the bridge sites between two adjacent Co sites. The water splitting step finishes among different surface Co sites. The two nearest neighboring *H are indeed adsorbing by the same Ni sites. Owing to the weak binding, the costs for simultaneously desorbing both $*H_2$ and $*OH^-$ finally have been compensated by the local lattice relaxation, which are all responsible for efficient H_2 generation.

To summarize, we have successfully demonstrated a unique method to prepare strongly coupled NiCoN/C nanocages through reacting ZIF-67 nanocubes with $Ni(NO_3)_2$ under sonication at room

temperature, followed by low temperature ammonolysis with NH_3. The strongly coupled NiCoN/C nanocages have awesome alkaline HER activity with the overpotential of 142 mV to reach the current density of 20 mA cm^{-2}, 34 mV smaller than that of Pt/C. Specifically, its mass activity reaches 0.204 mA/$\mu g_{cat.}$ at an overpotential of 200 mV, comparable to that of the commercial Pt/C (0.451 mA/$\mu g_{cat.}$). Moreover, the strongly coupled NiCoN/C nanocages also represent superior long-term stability. DFT calculations reveal that this originates from a high degree of amorphization urging C-sites to be an electron-pushing bath and promoting the electron-transfer with loss of orbital-selection-forbidden-rule among layers and sites. Strong (Ni, Co)-N bonding contributes to highly efficient electron transfers *via d-p-d* coupling to robustly transform Co^{2+} to Co^0, towards optimal initial water adsorption and splitting. Further orbital overlapping analysis indicates the final products exhibit an efficient desorption without encountering any over-binding with either Ni or Co sites to terminate the activities.

Supporting Information
Supporting Information is available from the Wiley Online Library or from the author.

Acknowledgements
J.P.L., B.L.H. and Y.G.C. contributed equally to this work. This work was financially supported by the National Natural Science Foundation of China (51671003), National Key Research and Development Program of China (No. 2016YFB0100201), BIC-ESAT funding and China Postdoctoral Science Foundation (No. 2017M620494).

Received: ((will be filled in by the editorial staff))
Revised: ((will be filled in by the editorial staff))
Published online: ((will be filled in by the editorial staff))

References

[1] S. Chu, A. Majumdar, *Nature* **2012**, *488*, 294.

[2] H. A. Gasteiger, N. M. Marković, *Science* **2009**, *324*, 48.

[3] M. K. Debe, *Nature* **2012**, *486*, 43.

[4] J. Lai, S. Guo, *Small* **2017**, *13*, 1702156.

[5] Y. Zheng, Y. Jiao, M. Jaroniec, S. Z. Qiao, *Angew. Chem. Int. Ed.* **2015**, *54*, 52.

[6] Y. Jiao, Y. Zheng, M. Jaroniec, S. Z. Qiao, *Chem. Soc. Rev.* **2015**, *44*, 2060.

[7] Q. Lu, Y. Yu, Q. Ma, B. Chen, H. Zhang, *Adv. Mater.* **2016**, *28*, 1917.

[8] X. Zou, Y. Zhang, *Chem. Soc. Rev.* **2015**, *44*, 5148.

[9] Y. Shi, B. Zhang, *Chem. Soc. Rev.* **2016**, *45*, 1529.

[10] D. Voiry, J. Yang, M. Chhowalla, *Adv. Mater.* **2016**, *28*, 6197.

[11] Y. Xu, M. Kraft, R. Xu, *Chem. Soc. Rev.* **2016**, *45*, 3039.

[12] J. Wang, F. Xu, H. Jin, Y. Chen, Y. Wang, *Adv. Mater.* **2017**, *29*, 1605838.

[13] Z. W. Seh, J. Kibsgaard, C. F. Dickens, I. Chorkendorff, J. K. Nørskov, T. F. Jaramillo, *Science* **2017**, *355*, 146.

[14] T. Wang, H. Xie, M. Chen, A. D'Aloia, J. Cho, G. Wu, Q. Li, *Nano Energy* **2017**, *42*, 69.

[15] L. Cheng, W. Huang, Q. Gong, C. Liu, Z. Liu, Y. Li, H. Dai, *Angew. Chem. Int. Ed.* **2014**, *53*, 7860.

[16] Q. Gong, Y. Wang, Q. Hu, J. Zhou, R. Feng, P. N. Duchesne, P. Zhang, F. Chen, N. Han, Y. Li, C. Jin, Y. Li, S.-T. Lee, *Nat. Commun.* **2016**, *7*, 13216.

[17] J. Lai, S. Li, F. Wu, M. Saqib, R. Luque, G. Xu, *Energy Environ. Sci.* **2016**, *9*, 1210.

[18] C. Tang, R. Zhang, W. Lu, L. He, X. Jiang, A. M. Asiri, X. Sun, *Adv. Mater.* **2016**, *29*, 1602441.

[19] J. Lai, B. Huang, Y. Tang, F. Lin, P. Zhou, X. Chen, Y. Sun, F. Lv, S. Guo, *Chem* **2018**, *4*, 1153.

[20] R. Subbaraman, D. Tripkovic, D. Strmcnik, K.-C. Chang, M. Uchimura, A. P. Paulikas, V. Stamenkovic, N. M. Markovic, *Science* **2011**, *334*, 1256.

[21] H. Yin, S. Zhao, K. Zhao, A. Muqsit, H. Tang, L. Chang, H. Zhao, Y. Gao, Z. Tang, *Nat. Commun.* **2015**, *6*, 6430.

[22] P. Wang, K. Jiang, G. Wang, J. Yao, X. Huang, *Angew. Chem. Int. Ed.* **2016**, *55*, 12859.

[23] X. Xu, Y. Chen, W. Zhou, Z. Zhu, C. Su, M. Liu, Z. Shao, *Adv. Mater.* **2016**, *28*, 6442.

[24] Y. Zheng, Y. Jiao, Y. Zhu, L. H. Li, Y. Han, Y. Chen, M. Jaroniec, S.-Z. Qiao, *J. Am. Chem. Soc.* **2016**, *138*, 16174.

[25] J.-X. Feng, H. Xu, Y.-T. Dong, X.-F. Lu, Y.-X. Tong, G.-R. Li, *Angew. Chem. Int. Ed.* **2017**, *56*, 2960.

[26] Z. Pu, I. S. Amiinu, Z. Kou, W. Li, S. Mu, *Angew. Chem. Int. Ed.* **2017**, *56*, 11559.

[27] K. Xu, H. Ding, M. Zhang, M. Chen, Z. Hao, L. Zhang, C. Wu, Y. Xie, *Adv. Mater.* **2017**, *29*, 1606980.

[28] J. Zhang, T. Wang, P. Liu, Z. Liao, S. Liu, X. Zhuang, M. Chen, E. Zschech, X. Feng, *Nat. Commun.* **2017**, *8*, 15437.

[29] H. Yan, Y. Xie, Y. Jiao, A. Wu, C. Tian, X. Zhang, L. Wang, H. Fu, *Adv. Mater.* **2018**, *30*, 1704156.

[30] Z. Zhu, H. Yin, C. T. He, M. Al‐Mamun, P. Liu, L. Jiang, Y. Zhao, Y. Wang, H. G. Yang, Z. Tang, D. Wang, X. M. Chen, H. Zhao, *Adv. Mater.* **2018**, *30*, 1801171.

[31] Y. Wang, B. Zhang, W. Pan, H. Ma, J. Zhang, *ChemSusChem* **2017**, *10*, 4170.

[32] Z. Xu, W. Li, Y. Yan, H. Wang, H. Zhu, M. Zhao, S. Yan, Z. Zou, *ACS Appl. Mater. Interfaces* **2018**, *10*, 22102.

[33] M. Zhou, Q. Weng, Z. I. Popov, Y. Yang, L. Y. Antipina, P. B. Sorokin, X. Wang, Y. Bando, D. Golberg, *ACS Nano* **2018**, *12*, 4148.

[34] C. Zhu, A.-L. Wang, W. Xiao, D. Chao, X. Zhang, N. H. Tiep, S. Chen, J. Kang, X. Wang, J. Ding, J. Wang, H. Zhang, H. J. Fan, *Adv. Mater.* **2018**, *30*, 1705516.

[35] Z. Jiang, Z. Li, Z. Qin, H. Sun, X. Jiao, D. Chen, *Nanoscale* **2013**, *5*, 11770.

[36] Z. Yao, A. Zhu, J. Chen, X. Wang, C. T. Au, C. Shi, *J. Solid State Chem.* **2007**, *180*, 2635.

[37] C. Ray, S. C. Lee, B. Jin, A. Kundu, J. H. Park, S. Chan Jun, *J. Mater. Chem. A* **2018**, *6*, 4466.

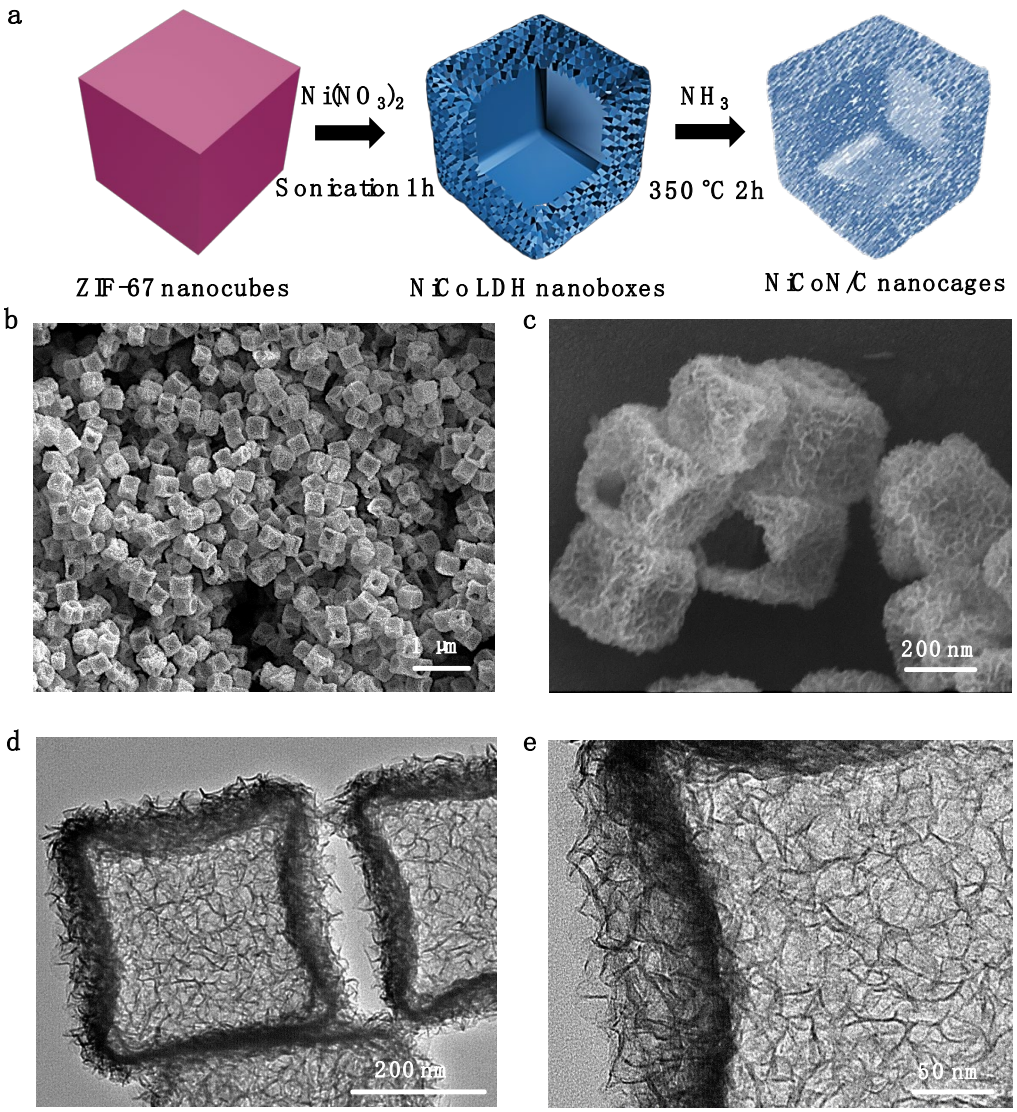

Figure 1. (a) Schematic illustration of the formation process of strongly coupled NiCoN/C nanocages. (b, c) FESEM and (d, e) TEM images of NiCo LDH nanoboxes.

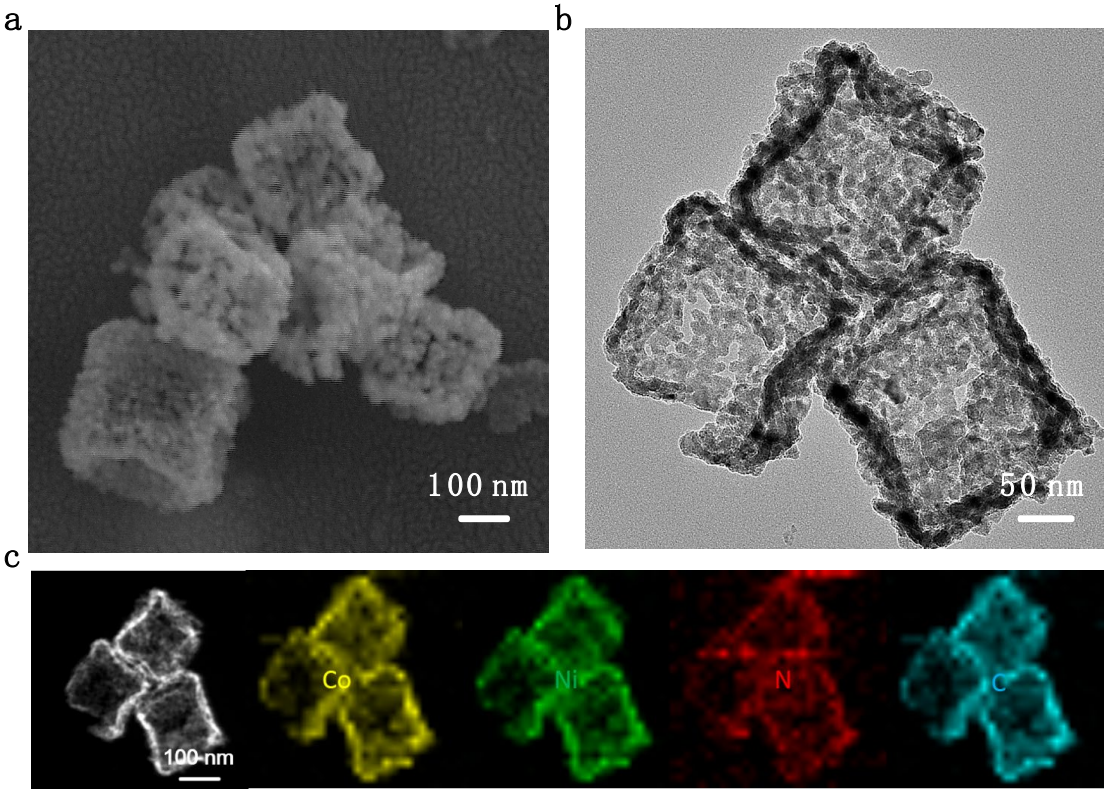

Figure 2. (a) FESEM image, (b) TEM image and (c) EDS elemental mapping image of strongly coupled NiCoN/C nanocages.

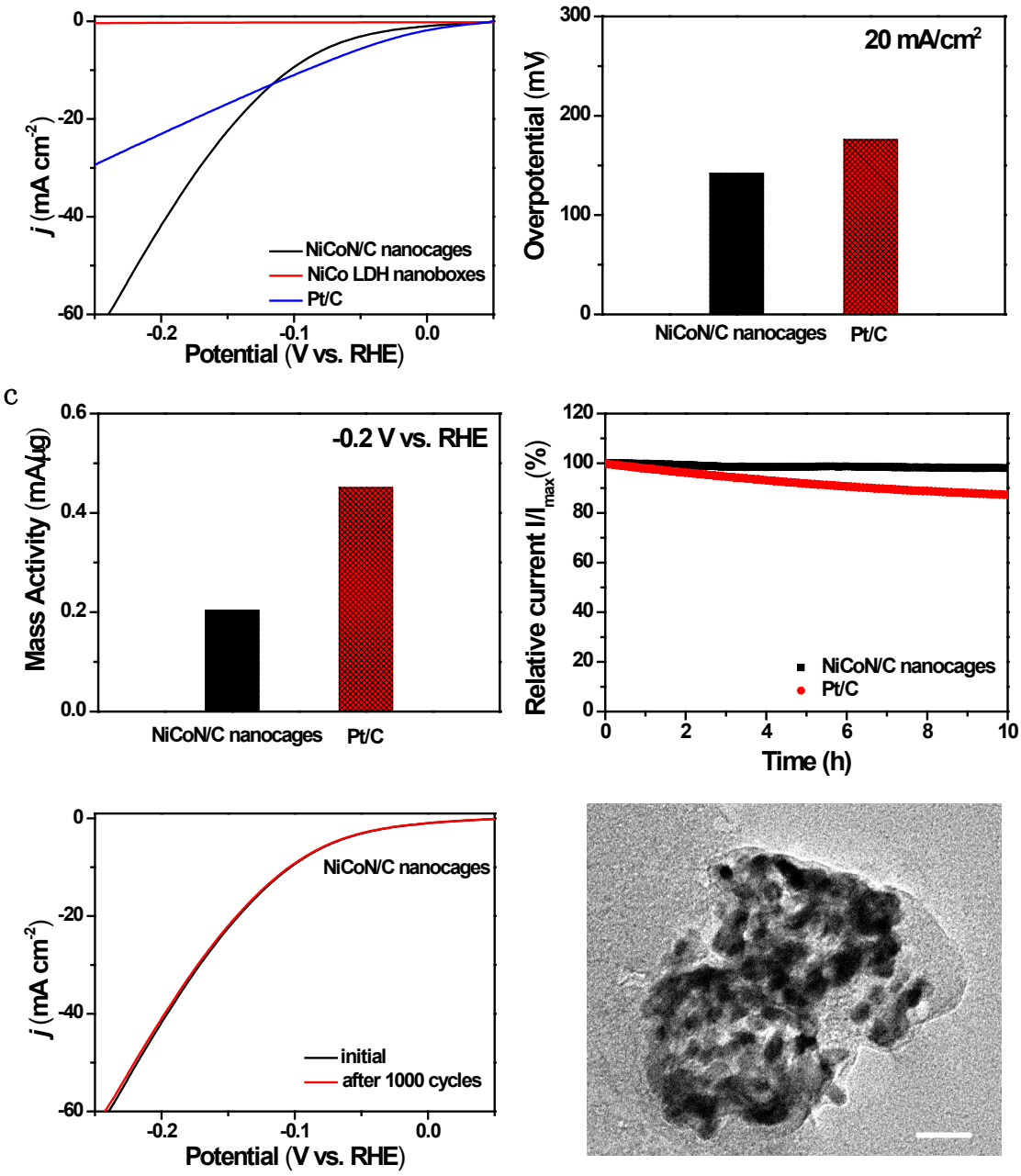

Figure 3. (a) HER polarization curve, (b) overpotential at 20 mA/cm^2, (c) mass activity at −0.2 V *vs* RHE of the strongly coupled NiCoN/C nanocages, NiCo LDH nanoboxes and Pt/C in 1.0 M KOH solution. (d) Chronoamperometry curves at overpotential of 200 mV of strongly coupled NiCoN/C nanocages and Pt/C, (e) HER polarization curves of strongly coupled NiCoN/C nanocages before and after 1,000 CV cycles and (f) TEM images of strongly coupled NiCoN/C nanocages after stability test.

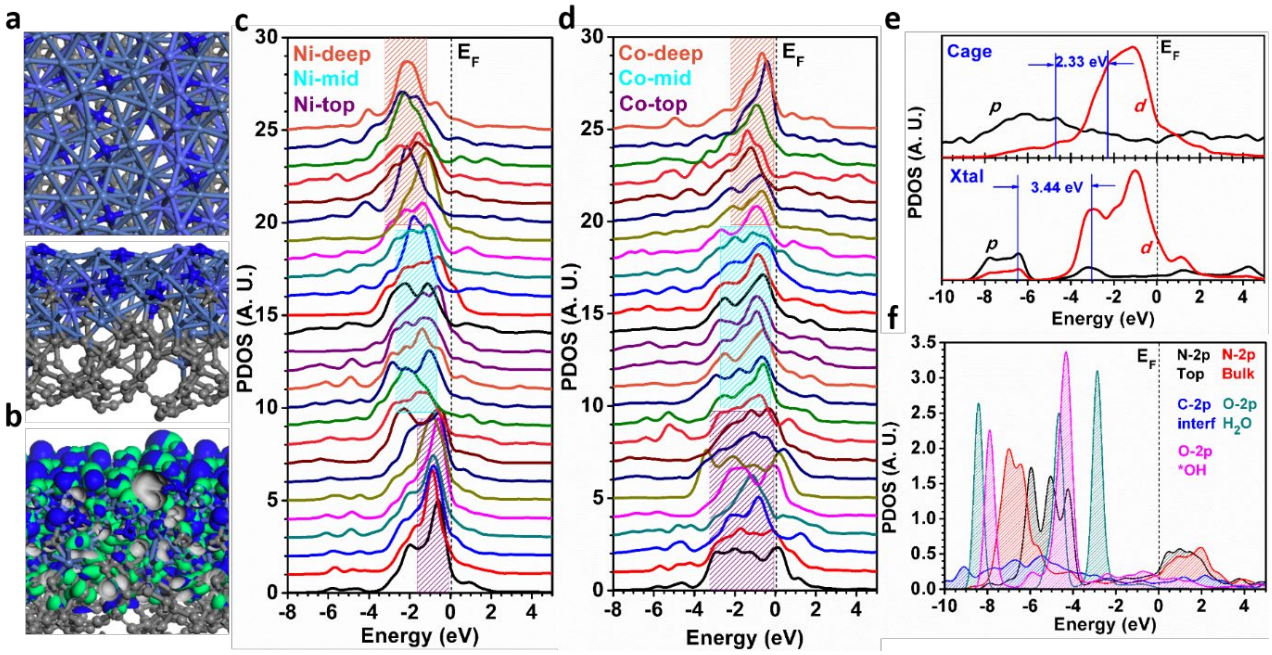

Figure 4. (a) The top-view (higher-panel) and side-view (lower-panel) of the NiCoN-C surface system. (b) The real-spatial contour plots for the bonding and anti-bonding orbitals near the E_F of the NiCoN-C system. (c) The evolutions of projected density of states (PDOSs) for the Ni-3d bands from different layer-depths of NiCoN-C surface model. (d) The evolutions of PDOSs for the Co-3d bands from different depths of NiCoN-C model. (e) The PDOSs for the overall p and d bands of NiCoN with (high-panel) and without (lower-panel) C-layer. (f) The PDOSs for different p-band covering ranges from surface-N, bulk-N, C-layer, $*OH^-$ and H_2O*, respectively.

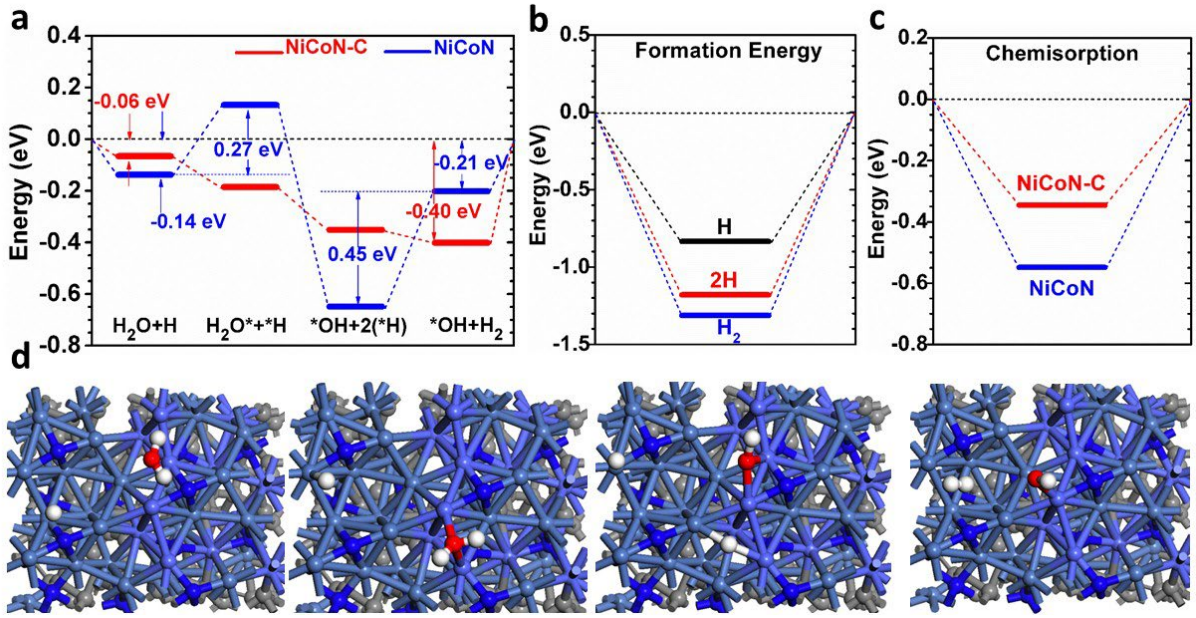

Figure 5. (a) Reaction energetic pathways for catalytic HER under alkaline condition between NiCoN-C and NiCoN surface systems. (b) The formation energies of H, 2H, and H_2. (c) The chemisorption energetic contrast for adsorbing H between NiCoN-C and NiCoN systems. (d) The evolutions of local structural configurations for illustrating HER process from NiCoN-C under alkaline condition.

The table of contents entry

A new family of nanocage materials (strongly coupled NiCoN/C nanocages) is rationally designed and synthesized *via* chemical etching of Co-based zeolitic imidazolate framework (ZIF-67) with $Ni(NO_3)_2$ at room temperature, followed by nitridation, which exhibit the Pt-like activity for hydrogen evolution reaction electrocatalysis in alkaline solutions.

Keyword: metal nitride; nanocages; carbon; MOFs; electrocatalysis

Jianping Lai, Bolong Huang, Yuguang Chao, Xu Chen, Shaojun Guo*

Strongly Coupled Nickel–Cobalt Nitrides/Carbon Hybrid Nanocages with Pt-like Activity for Hydrogen Evolution Catalysis